Multiplexed Analysis Using Time-Resolved Near-IR Fluorescence for the Detection of Genomic Material

Wieslaw J. Stryjewski,[1] Steven A. Soper,[1*] Suzzane Lassiter,[1] Lloyd Davis[2]
[1]Louisiana State University, Dep. Of Chemistry, Baton Rouge, LA 70803
[2]University of Tennessee, Space Institute, Tullahoma, TN 37388)

ABSTRACT

While fluorescence continues to be an important tool in genomics, new challenges are being encountered due to increased efforts toward miniaturization reducing detection volumes and the need for screening multiple targets simultaneously. We have initiated work on developing time-resolved near-IR fluorescence as an additional tool for the multiplexed analyses of DNA, either for sequencing or mutation detection. We have fabricated simple and compact time-resolved fluorescence microscopes for reading fluorescence from electrophoresis or DNA microarrays. These microscopes consist of solid-state diode lasers and diode detectors (SPADs) and due to their compact size, the optical components and laser head can be mounted on high-speed micro-translational stages to read fluorescence from either multi-channel capillary electrophoresis instruments or microfabricated DNA sorting devices. The detector is configured in a time-correlated single photon counting format to allow acquisition of fluorescence lifetimes on-the-fly during data acquisition in the limit of low counting statistics. In multiplexed analyses, lifetime discrimination serves as a method for dye-reporter identification using only a single readout channel. Also, coupled to multi-color systems, lifetime identification can significantly increase the number of probes monitored in a single instrument. In this work, near-IR fluorescence, including dye-labels and hardware, will be discussed as well as the implementation of near-IR fluorescence in DNA sequencing using slab gel electrophoresis and DNA microarrays.

1. INTRODUCTION

The developments in DNA sequencing have led to establishing fluorescence as a important identification tool in genomics. High sensitivity detection, especially in the single photon counting regime, allows reduction of the detection volumes to accommodate micro-separation platforms and their small volume requirements (< 1 nL). Typically the spectral differences of the labeling dyes are used in identifying the origin of the fluorescence from different targets. When DNA sequencing is carried out, four different dyes, one for each of the four nucleotide bases, are typically analyzed in separate detection channels. Efforts directed toward increased throughput has resulted in studies focused on the use of fluorescence lifetime discrimination techniques by several research groups using either time-resolved[1-5] or phase-resolved[6-9] methods to expand on the multiplexing capabilities of fluorescence. The use of a four-lifetime detection concept to calling bases in DNA sequencing has recently been described by Wolfrum et al[10]. In this work, rhodamine derivatives with absorption maxima at ~630 nm and lifetimes between 1.6 and 3.7 ns where used. These researchers demonstrated a read length of 660 bases with an estimated probability of correct identification equal to 90% in a single-lane/four-lifetime format, using capillary electrophoresis as the separation platform.

Soper and co-workers reported the use of time-resolved near-IR fluorescence in capillary gel electophoresis for a single base tract[2]. In this work, a C-tract was labeled with a tricarbocyanine derivative that was covalently attached to the 5' end of a M13 universal sequencing primer. The fluorescence lifetime of a series of electrophoretic peaks was found to be 581 ps +/- 9 ps in agreement with measurements of the same labeling dye measured under static conditions.

In many examples using fluorescence lifetime discrimination, only a single separation lane of the gel was interrogated. For high-throughput applications, it becomes necessary to perform the fluorescence measurement on many electrophoresis lanes either in a slab gel, multiple capillaries in an array machine or multi-channel microfabricated DNA sorting devices. We have recently developed a time-resolved fluorescence microscope that consists of a pulsed diode laser, producing 680 or 780 nm wavelength radiation with pulse widths of ~150 ps, single photon avalanche photodiodes (SPAD) and high numerical aperture microscope objectives. Two illumination configurations were used in these devices: (1) the laser head mounted under Brewster' angle with respect to the measured specimen[11]; (2) an epi-illumination format[12]. The ability to use diode lasers and avalanche photodiodes along with their small size allowed the

Biomedical Nanotechnology Architectures and Applications, Darryl J. Bornhop, et al., Editors,
Proceedings of SPIE Vol. 4626 (2002) © 2002 SPIE · 1605-7422/02/$15.00

optics, detector and laser to be mounted on the microscope body and situated it onto a microtranslational stage to allow rapid scanning of a slab gel or two-dimensional DNA microarray.

Due to the speed of the motion of the detector producing short integration times and the low load volume of material analyzed, low numbers of photocounts were accumulated into the fluorescence decay profiles. With lifetime identification strategies, the reproducibility in the measurements are crucial because identification is based on the ability to classify one of four different labels when DNA sequencing is being carried out. Therefore, the difference in lifetimes for a particular dye series should be spread by at least three standard deviation units. We have prepared a series of near-infrared (near-IR) tricarbocyanine dyes that exhibit properties favorable for multiplexing applications using time-resolved identification techniques[13]. These dyes are structurally similar and thus show similar absorption/emission maxima, 765/794 nm. The fluorescence lifetime within the series was controlled by incorporating a heavy atom modification into the molecular framework of the base chromophore. Incorporation of a single halide (I, Br, Cl, or F) or proton into a fixed location within the molecule structure provided means for variation of the lifetimes from 889 ps to 688 ps when measured in denaturing polyacrylamide gels. While these differences seem to be somewhat small, our previous studies have shown high precision using maximum likelihood estimation applied to capillary gel electrophoretic separation of near-IR labeled oligonucleotides[2,3].

In this manuscript we wish to discuss our results on the use of time-resolved near-IR fluorescence for reading signatures from DNA micro-arrays and base calling in DNA slab gel sequencing. For the DNA microarrays, probe oligonucleotides were covalently deposited onto a substrate and then, fluorescently-labeled complements added to the array and subsequently interrogated using time-resolved fluorescence detection. In the electrophoresis experiments, the time-resolved near-IR microscope was rastered over a slab gel and fluorescence from DNA sequencing fragments measured.

2. EXPERIMENTAL METHODS

2.1 Instrumentation. A schematic of the time-resolved near-IR scanner head in the Brewster's angle configuration is shown in Figure 1. The head consisted of a modified microscope extracted from a Li-COR 4000 automated DNA sequencer.[14] The laser (Picoquant GmbH model PDL 800) was mounted on the microscope head at an angle of 56^o with respect to the plane of the gel plates to minimize reflected radiation from being coupled into the optical system. The laser was operated at a lasing wavelength of 680 nm and a repetition rate of 80 MHz (pulse width = 100 ps, FWHM) with the output beam vertically polarized. The laser diode was driven by an electrical short-pulse generator, which supplied high-repetition rate picosecond current pulses to the diode head. The driver consisted of a radio-frequency pulse generator, a fast switch stage, a coax line driver and a pulse shaper stage.

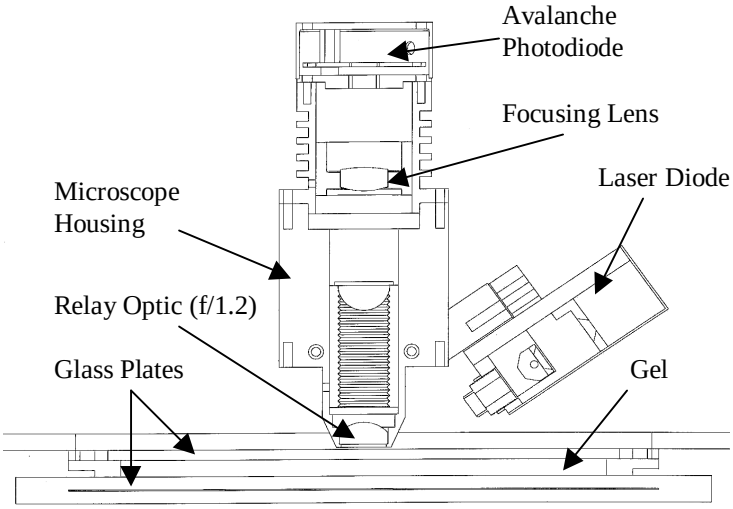

Figure 1. Schematic diagram of the time-resolved near-IR laser-induced fluorescence microscope head. The laser was mounted at 56^o with respect to the scanning surface to minimize light reflection from the glass surface. The laser used lased at 680 nm and used no temperature control.

The laser radiation was focused onto the surface of the gel plates using a f/1.4 lens that produced a spot on the gel of approximately 20 μm x 30 μm (elliptical beam shape of diode laser). The emission generated from the gel was subsequently collected by f/1.2 optics mounted in the microscope head and filtered with a single bandpass filter (center

wavelength = 710 nm; half band width = 20 nm). Following filtering, the emission was focused onto the face of an actively quenched, large photoactive area (id = 500 μm) avalanche photodiode operated in a Geiger mode for photon counting (PicoQuant SPM 200). The detector was also mounted on the microscope body at the secondary image plane of the relay optic set situated in the microscope. The dark count rate of this detector was determined to be 3500 cps and the count rate was linear with light intensity up to ~2.5 Mcps (dynamic range). The assembled microscope head was mounted on a linear stepper motor situated in the Li-COR 4000 automated DNA sequencer. Utilizing quadratic coded TTL signals to drive the scanner across the gel, the position of the head was decoded along with the direction of the movements and turnarounds. There were 400 pixels in each image line acquired at approximately 10 ms per pixel.

In the epi-illumination configuration of the time-resolved fluorescence microscope the components were mounted with the aid of a mounting cube and lens tubes purchased from ThorLabs (Newton, NJ). A circular aperture was placed in the secondary image plane of the objective to allow implementation of confocal imaging when required. The pulsed diode laser operated at a wavelength of 780 nm, a repetition rate adjustable from single shot to 80 MHz and a temporal pulse width of approximately 270 ps (FWHM) with 3.5 mW of average power. An integrated optics set was provided with the laser to produce an elliptically-shaped collimated output. The laser excitation beam was passed through a 780 nm line filter (Omega Optical, 780DF10, Brattleboro, VT), reflected by a dichroic filter (Omega Optical, 795DRLP) and focused onto the array surface using a 40X high numerical aperture (NA) microscope objective (Nikon, Natick, MA, NA=0.65). The $1/e^2$ spot size was measured to be 3 μm (minor axis) by 5 μm (major axis). The fluorescence excitation was collected by the same microscope objective, transmitted through the dichroic, a circular aperture set at 2.0 mm (clear diameter), and finally through a filter stack consisting of a long-pass filter (cut on wavelength = 830 nm, Newport Corporation, Irvine, CA) and a band-pass filter centered at 825 nm (825RDF30, Omega Optical). After passing through the filters, the fluorescence was focused onto the SPAD (SPCM-200, EG&G). The passively quenched SPAD possessed a photoactive area of approximately 180 μm in diameter. The dark count rate of this detector was about 200 cps. The entire fluorescence detector was mounted on an X/Y micro-translational stage driven by stepper motors interfaced to a PC computer. The step resolution of the stage was 12.7 μm with a scan range of 4 cm in both the X and Y directions. The scanner operated by taking a single step and then acquiring the fluorescence data for a software-selectable integration period (10 ms - 10 s).

The control and data acquisition software was developed using MicroSoft Visual Basic with some of the DLL libraries written in Visual C. A snapshot of the program screen in data acquisition mode is shown on Figure 2. Functionality of the program provides for recording the position of the scanning head and controlling bipolar stepper motors, streaming data to the hard drive (both intensity and time-resolved data), providing real-time visualization of the acquired images, and full interaction and programming of the single photon counting electronics (SPC 430, PicoQuant). During an experiment, data is stored in chunks of 2 GB and after completion of the run, the data was compressed one scan line at a time and assembled into one contiguous file. When the compressed binary file with the pixel decay information was opened, each line of the scan was decompressed separately and the 2D images (intensity and lifetime) generated. The line-by-line compression of the image was chosen for easy and fast access to the decay histograms on a pixel-by-pixel basis.

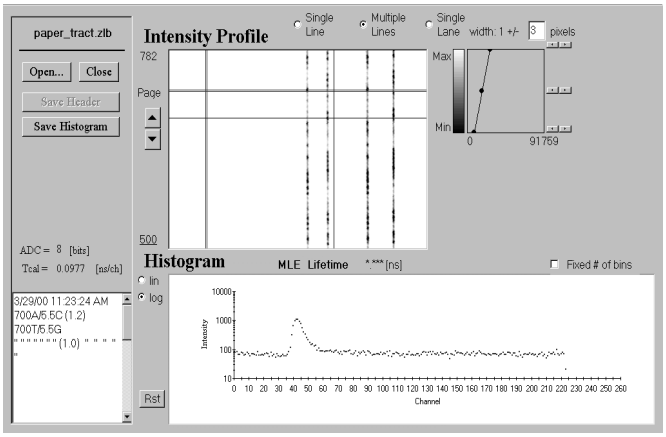

Figure 2. Front panel displays of the data analysis packages for analyzing time-resolved data from sequencing gels. Shown is the gel intensity image obtained from the time-resolved scanner. In this particular display, four lanes of sequencing data were imaged. The vertical and horizontal cursors (double line) defined a region on the gel from which the decay profile was constructed. In this region, no dye-labeled DNA was present and the resulting decay represents the instrument response function of the equipment.

2.2 Fluorescence lifetime calculations. The lifetimes of the image pixels were calculated using maximum likelihood estimation[15,16]:

$$1+(e^{T/\tau_f}-1)^{-1}-m(e^{mT/\tau_f}-1)^{-1}=\frac{\sum_{i=1}^{m} iN_i}{N_t}, \quad (1)$$

where N_t is the total number of photons in the decay profile, T is the time width of each bin, m is the number of bins over which the lifetime was calculated, i is the time bin index, τ_f is the lifetime, and N_i is the number of counts in the i^{th} time bin.

2.3 Reagents and methods for DNA sequencing. The gel plates consisted of boro-float glass that measured 21 cm (width) x 47 cm (length). The sieving gel was an 8%T (w/v) crosslinked gel (FMC Bioproducts Long-Ranger™, Rockland, ME) that contained 7.0 M urea as the denaturant and 1X TBE (pH = 8.0). The electrophoresis was typically run at –1 500 V for 12-24 h.

The two labeling dyes used for these experiments consisted of IRD700 (Li-COR Biotechnology, Lincoln, NE) and Cy 5.5 (Synthagen, Houston, TX), both of which were covalently attached to the 5' end of a M13 forward (-29) sequencing primer (17mer) through a C6 amino linker. The structures of the near-IR labeling dyes can be found elsewhere.[11] Their absorption and emission maxima where 685/705 and 675/694 nm, respectively, and are very similar, allowing efficient processing of the emission on a single channel and excitation with a single source. However, differences in the charge on the molecules did result in differences in their electrophoretic mobilities, requiring post-electrophoresis corrections during sequence assembly.

Sanger sequencing reactions were prepared using a modified procedure for the Amersham 7-deaza dye primer cycle sequencing kit employing an M13mp18 single-stranded DNA template. The sequencing reaction cocktail consisted of 5 pmol of the single stranded DNA template, 20 μL of TBE buffer, 1.0 μL of the appropriately labeled dye primer, 5 μL of double-distilled H_2O and 24 μL of the A,C,G or T extension mixture (Amersham Pharmacia Biotechnology, Piscataway, NJ). The sequencing reactions were performed in 1X TBE buffer (pH = 8.0). Cycle sequencing was accomplished in a PE series 2400 block thermal cycler (PE Applied Biosystems, Foster City, CA) using the following thermal cycling conditions (30 cycles); (i) 92°C for 2 s; (ii) 55°C for 30 s; (iii) 72°C for 60 s, followed by a final extension step at 72°C for 7 min. The primer concentration was reduced compared to the manufacturer's suggested protocol and the cycle number increased to reduce the amount of unextended primer remaining in the sequencing cocktail, which minimized smearing of unextended primer in the gel tract. The reaction cocktails were then subjected to a cold ethanol precipitation, which consisted of the addition of 7 μL of 7M NH_4OAc and 100 μL of 100% cold ethanol. The solution was then vortexed and placed in a freezer (4°C) for 30 min, followed by centrifuging for 30 min at 10 000 rpm at 4°C. The supernatant was removed by tapping the reaction vials on a counter top and then, thoroughly dried in a centro-vap for 1 h. Finally, the DNA pellet was reconstituted in a formamide loading solution, vortexed for 1 min and placed into a freezer until required for gel loading.

2.4 Reagents and methods for 2D DNA microarrays. All chemicals and solvents were purchased from Aldrich (Milwaukee, WI) and used as received. The near-IR dye used for these studies, IRD800 (Li-COR Biotechnology, Lincoln, NE) was used as received. Typically, stock solutions (0.1 mM) of the dye was made in DMSO and stored in a refrigerator (4°C) until required for use. The oligonucleotides used for hybridization assays were purchased from Midland Certified Reagent Company (Midland, TX) and consisted of a 5' amino modified end with a sequence of 5'$H_2N(CH_2)_6$-TTTTTTTTTTTTTTTGTCGTTTTACAAACGTCGTG-3'. The tethered oligonucleotide probe also contained a poly $(dT)_{15}$ linker to spatially remove the probe from the surface to improve its accessibility for hybridization.[17] The complement, which contained an near-IR label (IRD-800, Li-COR) possessed the following sequence: IRD800-5'CACGACGTTTGTAAAACGAC-3'.

Fluorescence measurements were performed by spotting IRD800 onto the surface of the appropriate substrate in a grid pattern defined by a piece of paper placed under the transparent substrate, with each element of the grid measuring 2 mm x 2 mm (5 x 5 array). The dye was dissolved in DMSO and spotted onto the surface using a 25 μm i.d. capillary. The total volume of dye deposited for each spot was estimated to be approximately 1.0 μL with the diameter of the spot

being approximately 2 mm. After spotting, the slides were either allowed to dry (in the dark) under a stream of N_2 or covered with a cover slip. The procedures of covalent attachment and surface quantification of oligonucleotides onto the substrate and hybridization assays have been discussed elsewhere.[12]

3. RESULTS AND DISCUSSION

3.1 Scanning gel plates for DNA sequencing. Using equation (1), the lifetimes for both the IRD700 and Cy5.5-labeled G-tracts were determined. The average lifetime value for the IRD700-labeled fragments was found to be 718 ps with a standard deviation of 5 ps (relative standard deviation = 0.7%), while for the Cy5.5-labeled fragments, τ_f was 983 ps with a standard deviation of 13 ps (relative standard deviation = 1.3%). By integrating the area under the decay profiles, the average number of photocounts included in the lifetime calculations were found to be (background corrected) 56 500 counts for the IRD700-labeled fragments and 45 750 counts for the Cy5.5 fragments. For maximum likelihood estimation of the lifetime, the standard deviation can be determined from $\tau_{f(avg)} \times N_t^{-1/2}$, where N_t is the total number of photoelectrons included in the calculation and $\tau_{f(avg)}$ is the average calculated lifetime. Calculation of the standard deviation based on the photocount numbers was 3 ps (IRD700) and 5 ps (Cy5.5), in close agreement to the standard deviations obtained from the actual measurements. This indicates that the variances in the lifetime measurements are determined primarily by photon statistics and not instrumental or background artifacts, a direct consequence of using near-IR fluorescence monitoring. Using these means and standard deviations, a student's t test indicated that we could successfully discriminate between these two dyes at > 99% confidence interval ($n_{obs} = 141$; $t_{calc} = 174$; $t_{99\%} = 2.58$).

To evaluate the efficiency in base-calling using our lifetime approach, we performed a two-dye/two-lane sequencing experiment, in which the A (IRD700 label) and T (Cy5.5 label) tracts were run in one lane and the C (IRD700 label) and G (Cy5.5 label) in another lane. The efficiency of our base-calling was compared to a single-dye sequencing run, in which the four terminal bases were run in separate lanes of the gel using a single dye-labeled primer (Cy5.5-labeled sequencing primer). Since it was found that the Cy5.5-labeled fragments migrated at a slightly higher rate as that of the IRD700-labeled fragments, the identified IRD700 bands were frame shifted across the entire tract. To assist in identifying the number of components comprising a band and securing proper overlap between the two tracts, the base-calling algorithms associated with this machine were first implemented, which identified peaks as either A's or C's in each tract and then overlaying the data from each tract. Following this process, the A's were then identified as either A or T and the C's as either C or G using lifetime discrimination. In addition, the terminal base identification for a series of bands with poor electrophoretic resolution were carefully evaluated by obtaining lifetime patterns across these bands on a pixel-by-pixel basis.

Table 1. Read accuracies and errors as a function of read length using a single-dye/four-lane and a two-dye lifetime/two-lane sequencing strategies. The data was accumulated on the automated Li-COR 4000 DNA sequencer using slab gel electrophoresis.

Read length (bp)	Insertions	Deletions	Miscalls	Read Accuracy
Single-dye/four-lane				
550	1	0	3	99.3%
600	9	3	4	97.3%
670	21	4	4	95.7%
Two-dye lifetime/two-lane				
550	0	0	2	99.7%
600	0	0	2	99.7%
670	0	0	2	99.7%

A single-dye/four-lane format was used to construct the sequence of an M13mp18 template with the called bases compared directly to the known sequence of the M13mp18 phage and the known priming site. The single-dye/four-lane method served as a standard for comparing the efficiency of our lifetime base call approach, since the single-dye/four-lane method uses no spectroscopic identification process for calling the bases and the read accuracy depends primarily on the resolution in the electrophoresis. For the single-dye/four-lane sequencing run, the bases were called using the automated algorithms developed for this machine by the manufacturer. For a read length which included 670 bases, the

total number of errors were found to be 29, resulting in a read accuracy of 95.7% (see Table 1). As can be seen from the data in Table 1, the majority of the errors were insertion errors, typically resulting from spacing artifacts due to poor electrophoretic efficiency for the latter migrating fragments. If the read was dropped to 600 bases, the accuracy improved to 97.3%, while a read length of 550 bases produced a read accuracy of 99.3% due primarily to a reduction in insertion/deletion errors.

The bases were then called from a two-dye/two-lane format with the two bases in the single tract called using lifetime discrimination methods. The terminal bases A/T were run in one lane and C/G in another. The results on the number and type of errors as a function of read length are presented in Table 1. The bases were called by selecting the center pixel of a band (t = 10 ms) and constructing a decay profile over this integration period from which the lifetime was calculated using equation (1). In the case of poor electrophoretic resolution (R < 0.5) for a series of bands, the lifetimes were calculated over 10 ms pixels across the bands and the resulting pattern used to identify the terminal bases. As can be seen from Table 1, the read accuracy was found to be better than the single-dye/four-lane strategy due to the fact that fewer insertion and deletion errors were uncovered during sequence reconstruction. We found that the number of miscalled bases from the primer annealing site was equal to 2 for a read length of 670 bases, similar to that found for the miscall number obtained in the single-dye/four-lane approach. The number of miscalls would be expected to increase based on the fact that in the lifetime call, a spectroscopic measurement is required to identify one of two terminal bases, which should add errors to the identification process. These results indicate that the lifetime approach as implemented here produces very high efficiency in the spectroscopic identification process. The reduction in insertion and deletion errors using lifetime patterning was a consequence of increased information content in the electrophoretic bands experiencing poor electrophoretic resolution.

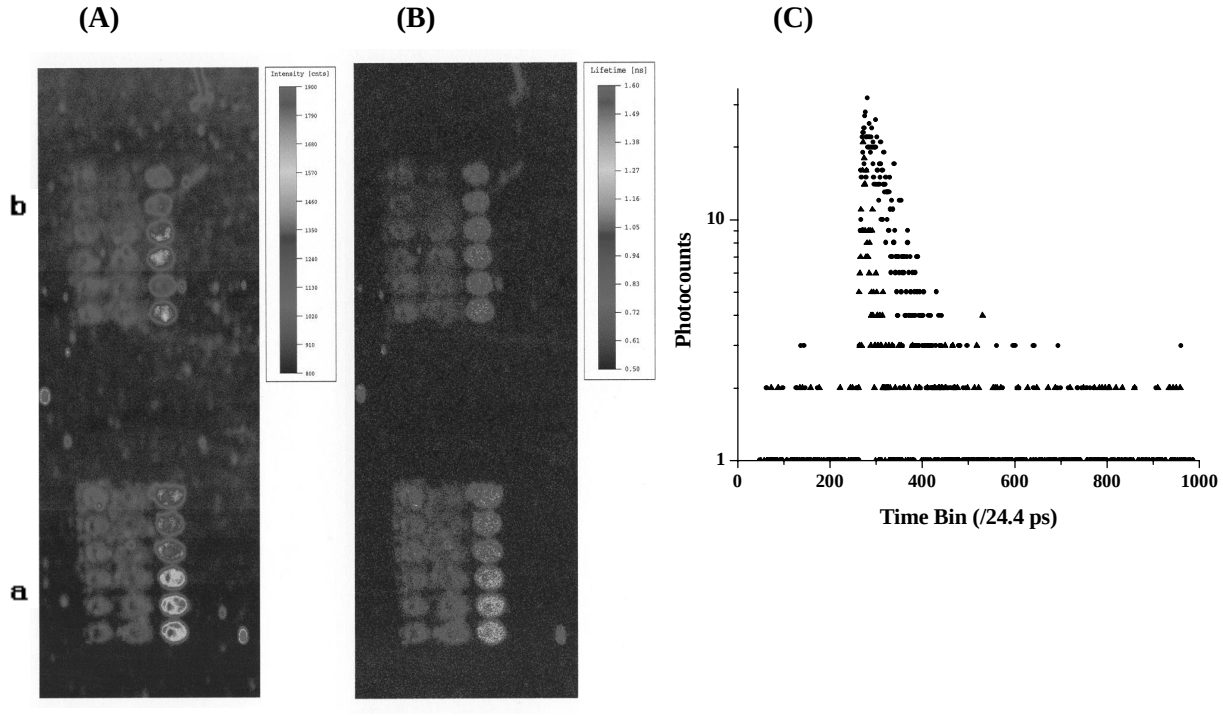

Figure 3. Fluorescence intensity image (A) and lifetime image (B) of 2, 4 x 6 DNA micro-arrays (a and b). The spots were approximately 400 μm in diameter with a center-to-center spacing of 600 μm. (C) Decay profiles for background generated from substrate (triangles) and a hybridization spot (array (a), column 1, circles) for a single image pixel.

3.2 DNA hybridization on PMMA substrates with time-resolved near-IR fluorescence. We next investigated our ability to analyze hybridization events using time-resolved fluorescence of near-IR-labeled oligonucleotide complements of tethered DNA oligonucleotide probes to a surface. The results of these experiments are depicted in Figures 3 and 4 with Figure 3A showing the intensity image and Figure 3B the lifetime image of 2, 4 X 6 DNA micro-arrays. To acquire the images, the scanner was moved in 12.7 μm steps and the integration time per pixel was 0.1 s. From the data shown for both the intensity and lifetime images, it was determined that each spot was circular with an average diameter of 35 pixels (spot diameter = 444 μm). In these experiments, four columns (six spots per column) are present in the array; (1) fully matched duplexes; (2) three-base mismatch; (3) one-base mismatch and; (4) fully mismatched duplexes. As can be seen from the intensity or lifetime image, little non-specific adsorption of DNA to the surface was observed. Also, using our hybridization conditions, the fluorescence intensity (see Figures 3A and 4A) for column 1 (fully-matched duplexes) was higher than that seen in columns 2-4.

By integrating the background-corrected intensity (background-corrected with respect to column 4) over each spot of the array (1018 pixels), the average intensity was determined to be 8.1 (∀ 2.0) x 10^5 counts for column 1, 3.8 (∀ 0.4) x 10^5 counts for column 2 and 4.1 (∀ 0.3) x 10^5 counts for column 3. Using the background-corrected counts for only column 1 and the integrated background counts per spot (7.6 x 10^5), the SNR was found to be 9.3 x 10^2, where the SNR was calculated from SNR = $S/(B)^{1/2}$, where S is the background-corrected signal and B is the background. Each spot (area = 1.6 x 10^5 μm^2) contains 5.1 x 10^{-17} moles of labeled-oligonucleotides. Our mass detection limit (SNR = 2) for a typical spot using near-IR fluorescence following DNA hybridization is 1.0 x 10^{-19} moles (0.38 molecules/μm^2).

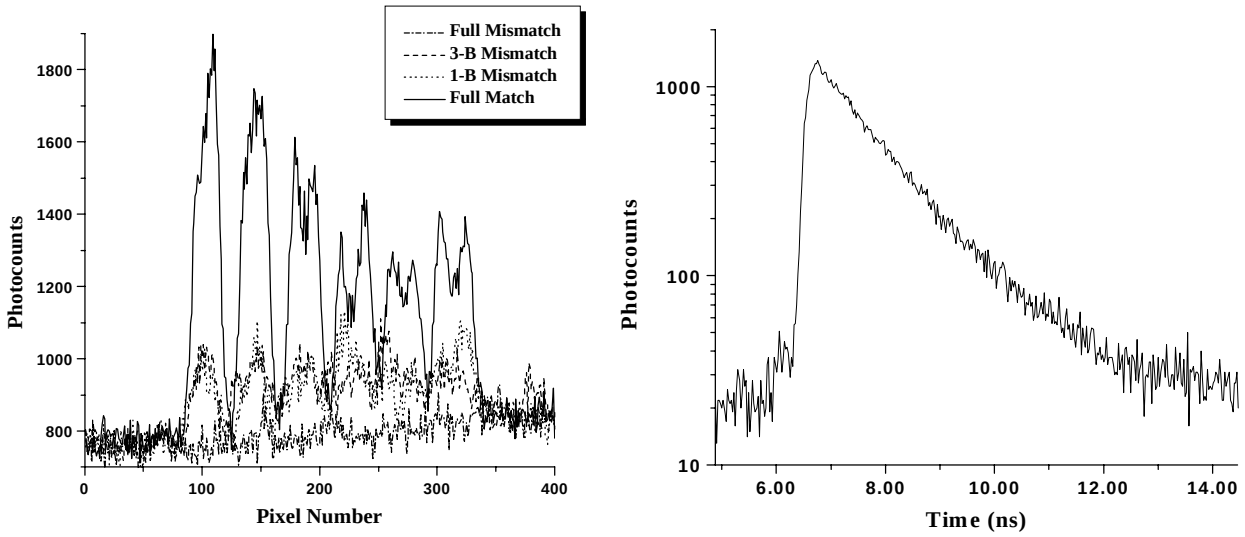

Figure 4. (A) Fluorescence intensity of the 4-columns of the DNA micro-array (perfect match, 1-base mismatch, 3-base mismatch, and fully mismatched duplexes) interrogated using time-resolved near-IR fluorescence. The intensity represents one pixel taken from the center of each column of array (a) (see Figure 3A). (B) Decay profile taken from a complete-matched hybridization spot (column 1, array (a), see Figure 3).

We also obtained the image of this hybridization array using time-gated detection. The position of the time-gate was selected to effectively discriminate the scattered photons from the fluorescence photons (see Figure 3B). When the array was re-imaged using time-gated detection (data not shown), we found that the SNR improved 10-fold (LOD = 0.038 fluors/μm^2) compared to the SNR obtained for the image depicted in Figure 3A.

We next carried out a lifetime analysis during imaging using maximum likelihood estimators (see equation 1) and this lifetime image is shown in Figure 3B. Comparison of the lifetime image to the intensity image over the entire array surface showed qualitatively that the lifetime image was much cleaner in terms of fewer high intensity/lifetime spots, which show up in non-hybridization pixels of the image. These spots arise from imperfections in the substrate material, which scatter light increasing the intensity at that pixel. However, in the lifetime image these spots do not show up due to the fact that the calculated lifetime is partially immune to scattering increases since the time distribution of these

photons are coincident with the laser pulse and the lifetime was calculated over a time interval where the scattered photon contribution to the decay is minimal. We also noticed that the lifetime image contained a wide spread of values when comparing the lifetimes of spots between columns. Since the only distinction between columns is the number of labeled targets present in a spot resulting from mismatches, we would anticipate similar lifetime values between columns of the array due to the concentration independent behavior of the lifetime when implementing lifetime imaging techniques.[18,19] As can be seen in Figure 3C, the number of photons in the fluorescence decay (accumulated on a single pixel) were small (~1550 counts) and the background makes a significant contribution to the resulting decay. Since our algorithm makes no distinction between multi-exponential decays and single exponential decays, the poor photon statistics and large background contribution biases in the lifetime determination, resulting in the lifetime discrepancies observed between columns.[20]

4. CONCLUSIONS

Simple instrumental modifications were required to allow implementation of time-resolved fluorescence in a conventional automated DNA sequencer. This indicates that many existing machines, which use steady-state fluorescence, can be easily configured to do time-resolved fluorescence as well to increase system capabilities. Our data indicates that the accuracy in the lifetime identification was high due to the use of near-IR fluorescence excitation, which minimizes impurity fluorescence generated from the sample matrix, minimizing variations in the calculated lifetimes. In addition, due to the high sensitivity of near-IR fluorescence, short integration times can be used to construct decay profiles across poorly resolved bands allowing a lifetime pattern analysis, which can assist in elucidating components comprising the bands.

We also have built a device for near-IR time-resolved fluorescence detection and imaging of solid surfaces for reading fluorescence signatures from DNA micro-arrays. The timing response of this device was found to be 275 ps, which was adequate for determining sub-nanosecond fluorescence lifetimes. Additionally, we found that the LOD of this device was 0.38 molecules/μm^2 and could be improved by a factor of 10 using time-gated detection.

ACKNOWLEDGMENTS

The authors would like to thank the National Institutes of Health (HG-001499-04, HG01182-03, R01-01499, and R23-CA84625), and FMC BioProducts (Rockport, ME) for financial support of this work.

REFERENCES

1. Bachteler, G.; Drexhage, K.-H.; Arden-Jacob, J.; Han, K.-T.; Kollner, M.; Muller, R.; Sauer, M.; Seeger, S.; Wolfrum, J. *J. Luminesc.* **1994**, *62*, 101-108.
2. Soper, S.A.; Legendre, B.L.; Williams, D.C. *Anal. Chem.* **1995,** *67*, 4358-4365.
3. Soper, S.A.; Flanagan, J.H.; Legendre, B.L.; Williams, D.C.; Hammer, R.P. *IEEE J. Sel. Top. Quant. Electr*. **1996,** *2*, 1129-1139.
4. Sauer, M.; Arden-Jacob, J.; Drexhage, K.H.; Marx, N.J.; Karger, A.E.; Lieberwirth, U.; Muller, R.; Neumann, M.; Nord, S.; Schulz, A.; Seeger, S.; Zander, C.; Wolfrum, J. *Biomed. Chromatogr.* **1997**, ***11***, 81-82.
5. Flanagan, J.H.; Owens, C.V.; Romero, S.E.; Waddell, E.; Kahn, S.H.; Hammer, R.P.; Soper, S.A. *Anal. Chem.* **1998**, *70*, 2676-2684.
6. Nunnally, B.K.; He, H.; Li, L.C.; Tucker, S.A.; McGowen, L.B. *Anal. Chem.* **1997**, *9*, 2392-2397.
7. Li, L.C.; He, H.; Nunnally, B.K.; McGowen, L.B. *J. Chromatogr.* **1997,** *695*, 85-92.
8. He, H.; Nunnally, B.K.; Li, L.C.; McGowen, L.B. *Anal. Chem.* **1998,** *70*, 3413-3418.
9. Li, L.; McGowen, L.B. *J. Chromatogr.* **1999**, *841*, 95-103.
10. Lieberwirth, U.; Arden-Jacob, J.; Drexhage, K.H.; Herten, D.P.; Muller, R.; Neumann, M.; Schulz, A.; Siebert, A.; Siebert, S.; Sagner, G.; Klingel, S.; Sauer, M.; Wolfrum, J. *Anal. Chem.* **1998**, *70*, 4771-4779.
11. Lassiter, S.J.; Stryjewski, W.J.; Legendre, B.L.Jr.; Erdmann, R.; Wahl, M.; Wurm, J.; Peterson, R.; Middendorf, L.; Soper, S.A. *Anal. Chem.* **2000,** 72, 5373-5382
12. Waddell, E.; Wang, Y.; Stryjewski, W.J.; McWhorter, S.; Henry, A.C.; Evans, D.; McCarley, R.L.; Soper, S.A. *Anal. Chem.* **2000,** 72, 5907-5917
13. Flanagan, J.H.; Owens, C.V.; Romero, S.E.; Waddell, E.; Kahn, S.H.; Hammer, R.P.; Soper, S.A. *Anal. Chem.* **1998**, *70*, 2676-2684.

14. Middendorf, L.R.; Bruce, J.C.; Eckles, R.D.; Grone, D.L.; Roemer, S.C.; Sloniker, G.D.; Steffens, D.L.; Sutter, S.L.; Brumbaugh, J.A.; Patonay, G. *Electrophoresis* **1992**, *13*, 487-494.
15. Soper, S. A.; Legendre, B. L. *Appl. Spectrosc.* **1994**, *48*, 400-405.
16. Hall, P.; Selinger, B. *J. Phys. Chem.* **1981**, *45*, 2941-2946.
17. Guo, Z.; Guilfoyle, R. A.; Thiel, A. J.; Wang, R.; Smith, L. M. *Nucl. Acids Res.* **1994**, *22*, 5456-5465.
18. Lakowicz, J.R.; Szmacinski, H.; Nowaczyk, K.; Johnson, M.L. *PNAS* **1992**, *89*, 1271-1275.
19. Lakowicz, J.R.; Szmacinski, H.; Nowaczyk, K.; Berndt, K.W.; Johnson, M. *Anal. Biochem.* **1992**, 202, 316-330.
20. Soper, S. A.; Legendre, B. L. *Appl. Spectrosc.* **1998**, *52*, 1-6.